ELSEVIER

Journal of Molecular Catalysis A: Chemical 135 (1998) 187–197

JOURNAL OF MOLECULAR CATALYSIS A: CHEMICAL

Inverse gas chromatography studies of alkali cation exchanged X-zeolites

Jinhai Xie, Mosto Bousmina, Guoying Xu, Serge Kaliaguine *

Department of Chemical Engineering, Laval University, Ste-Foy, Quebec, Canada G1K 7P4

Received 23 September 1997; accepted 21 November 1997

Abstract

The base strength of alkali cation exchanged X-zeolites was investigated using the IGC technique. The results show that IGC can give information about the acid–base interaction with polar probe molecules. The specific interaction (I^{sp}, mJ/m^2) between zeolites and benzene, toluene, chloroform can be correlated to the strength of acid–base interaction.

Keywords: Zeolites; Basicity; Acidity; Inverse gas chromatography; Specific interaction; Benzene; Toluene; Chloroform

1. Introduction

The Inverse Gas Chromatography (IGC) technique, which can be traced to 1967 [1] with subsequent development of the theory and methodology in 1969 [2], is one of the frequently used techniques in material science. The initial application of IGC was only in the study of synthetic polymers. Today, IGC is widely utilized to study synthetic and biological polymers, copolymers, polymer blends, glass and carbon fibers, coals, foods [3] and carbon blacks [4].

IGC is designed for analysis of the stationary solid phase within a column. This is in contrast to GC which is used to separate and analyze the compounds of an injected gas mixture pulse. In IGC, the injected molecules, called probes, should be the only component of the pulse. The probes are introduced into the column to investigate their interactions with the solid surface of the packing material. Except for the reversal of roles of the mobile and stationary phases, the theoretical principles and instruments are basically the same as for traditional GC.

The information one can obtain from IGC experiments are the various properties of the stationary phase, such as transition temperatures, polymer–polymer interaction parameters, acid–base characteristics, solubility parameters, crystallinity, surface tension, and surface area [3]. In vapor–solid systems, IGC can also give informations about the adsorption properties, heats of adsorption, interaction parameters, interfacial energy, and diffusion coefficients.

* Corresponding author.

1381-1169/98/$ - see front matter
PII: S1381-1169(97)00303-8

Up to now, only one paper has described the application of the IGC technique to zeolites for measuring adsorption isotherms of several hydrocarbons over zeolite 4A [5]. This technique has, however, the potential advantage of allowing an easy characterization of the various interactions between the surface and the probe at rather high temperatures. Base catalyzed reactions performed over ion exchanged zeolites are usually conducted at temperatures exceeding 200°C. On the other hand, the probes that are usually employed for the characterization of basic strength (pyrrole, benzene, chloroform) by such techniques as FTIR [6–17], XPS [18–20] and microcalorimetry [21] are essentially desorbed at temperature well below 100°C. Thus, when these molecules are involved in a catalytic process, their interactions with the basic sites of the zeolites may be different from the ones involved in the steady adsorbed state. IGC has the potential of reflecting the various interactions of these gaseous molecules with the catalytic surface in working conditions. To our knowledge, no paper has mentioned the application of IGC to the characterization of zeolite base and/or acid strength.

This work was thus undertaken in order to investigate how IGC may be applied to estimate the various interactions between benzene, toluene or chloroform and the Lewis base sites of alkali exchanged X-zeolites.

2. Experimental

2.1. Materials

Various alkali metal cation-exchanged X-zeolites have been prepared from the sodium form (20 g) contacted with the corresponding chloride solutions. The exchange temperature was maintained at 70–80°C and the time for a single exchange was 24 h. Up to three successive exchanges were performed in order to obtain high exchange levels. After each ion exchange, the zeolite (20 g) slurry was filtered and washed with 500-ml hot deionized water (about 50–60°C) for three times, followed by drying at 120°C overnight. The unit cell chemical composition of all samples was determined by atomic absorption spectroscopy. The analysis results are shown in Table 1.

Table 1
The unit cell composition of zeolites

Zeolites	Unit cell composition
LiX	$Li_{80}Na_{5.4}(AlO_2)_{85.4}(SiO_2)_{106.6}$
NaX	$Na_{85.4}(AlO_2)_{85.4}(SiO_2)_{106.6}$
KX	$K_{68.9}Na_{16.5}(AlO_2)_{85.4}(SiO_2)_{106.6}$
RbX	$Rb_{60.9}Na_{24.5}(AlO_2)_{85.4}(SiO_2)_{106.6}$
CsX	$Cs_{61.5}Na_{23.9}(AlO_2)_{85.4}(SiO_2)_{106.6}$

2.2. BET specific surface measurement

The BET surface area was determined by nitrogen adsorption using an OMNISORP-100 instrument at relative pressure $P/P^0 \leq 0.1$. The external surface area of zeolites was calculated from the *t*-plot diagram [22].

2.3. Inverse gas chromatography

Zeolite powders were pressed, then gently crushed and a fraction with particles diameter between 500–600 μm was separated by sieving. About 20 mg of zeolite particles were filled into a 5-cm length of stainless steel column with an inside diameter of approximately 2.07 mm. To begin packing the column, silane-treated glass wool was used to plug one end of the column, and this same end was attached to a water suction pump. A precisely weighed amount of zeolite particles was put into the column and the packing was accomplished with the aid of a mechanical vibrator. The other end of the column was then also plugged with silane-treated glass wool. Then, the column was placed in the chromatograph with its only inlet port connected, as the zeolite packing was dehydrated at 200°C overnight under a helium flow

of 30 ml/min. The IR spectra of all samples were recorded at room temperature using KBr wafers with 3 wt.% of zeolite, to check for the presence of chemisorbed CO_2. No peak was observed neither in the 2000–2500 cm^{-1} nor in the 1300–1500 cm^{-1} region, which excludes the possibility of any significant coverage of the basic sites by CO_2 in these samples.

An HP 5890 gas chromatograph equipped with a flame ionization detector and an HP 3390 integrator was employed for the IGC experiments. The measurement temperature range was from 200°C to 280°C. Helium was used as the carrier gas. HPLC-grade *n*-alkane probes and other polar molecules were purchased from Aldrich Chemical, and they were used as received. A Hamilton gas-tight syringe (5 μl) was used throughout the experiments. Typically, 0.3–0.5 μl of the probe vapor was aspirated from the vial of probes, and injected in the GC. Methane was used as a marker. At least three injections of each probe were carried out, and the retention times were measured at the peak maximum.

For each probe and at each temperature studied, the retention time measurement was first performed at various carrier gas flow rates. The data were only treated when the flow rate was high enough so as not to affect the retention volume. On this basis, the carrier gas flow rate was chosen as 100 ml/min for benzene and toluene and as 65 ml/min when chloroform was the probe.

3. Calculations

The net retention volume V_n was calculated from the following equation [23]:

$$V_n = Fj(t_r - t_m)CT \tag{1}$$

where F = uncorrected flow rate detected by timing a soap film; t_r = retention time of the given probe; t_m = retention time of a non-adsorbing marker (methane); j = James–Martin factor for the correction of gas compressibility under pressure difference between column inlet (P_{in}) and outlet (P_{out}), estimated as:

$$j = \frac{3}{2}\frac{\left[\frac{P_{in}}{P_{out}}\right]^2 - 1}{\left[\frac{P_{in}}{P_{out}}\right]^3 - 1} \tag{2}$$

$$C = 1 - \frac{P_{H_2O}}{P_{out}} \tag{3}$$

where P_{H_2O} is the water pressure in the bubble flowmeter.

$$T = \frac{T_{col}}{T_{meter}} \tag{4}$$

When adsorption takes place in the Henry's Law region, i.e., at infinite dilution, the standard free energy of transferring one mole of vapor from a gas phase (at a pressure of 101 kPa) to a standard state on the surface, designated as the variation in the standard free energy of adsorption ΔG_{ads} is given by the following equation [24]:

$$\Delta G_{ads} = -RT_{col}\ln\left[\frac{P_{out}V_n}{\pi_0 Sm}\right] \tag{5}$$

where R is the ideal gas constant, T_{col} is the column temperature, V_n is the net retention volume, P_{out} is the column outlet and π_0 is the spreading pressure of the adsorbed film in the De Boer standard state (338 μN/m). S is the specific surface area, here the external surface area and m is the weight of the zeolite samples.

The dispersive component of the surface energy (γ_s^D) can be obtained from the following equation [23]:

$$\gamma_s^D = \frac{1}{4}\frac{\Delta G_{CH_2}^2}{\gamma_{CH_2} N^2 a_{CH_2}^2} \tag{6}$$

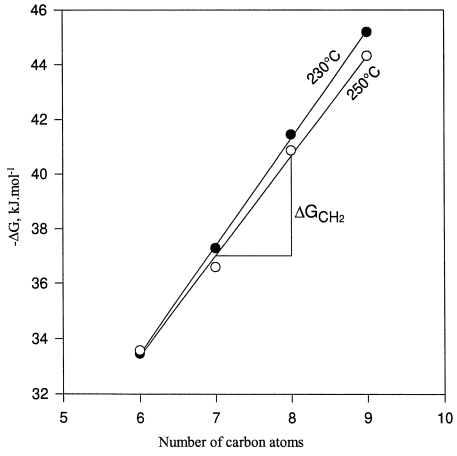

Fig. 1. The variation of adsorption free energy of alkanes vs. number of carbon atoms, NaX.

where N is Avogadro's number, a_{CH_2} is the area occupied by a $-CH_2-$ group (0.06 nm^2) [23] and γ_{CH_2} is the surface tension of a surface consisting of CH_2 groups [23].

$$\gamma_{CH_2} = 35.6 + 0.058(20 - T_{col})\,\text{in mJ/m}^2, \quad (7)$$

while for each adsorbent, the (ΔG_{CH_2}) can be obtained from the slope of the graph ΔG_{ads} vs. number of carbons for different *n*-alkanes (Fig. 1).

The specific interaction (I^{sp}, e.g., of polar probes) can be obtained from the difference of the free energy of adsorption ($\Delta\Delta G$) between a polar probe and the real or hypothetical *n*-alkane with the same surface area (Fig. 2).

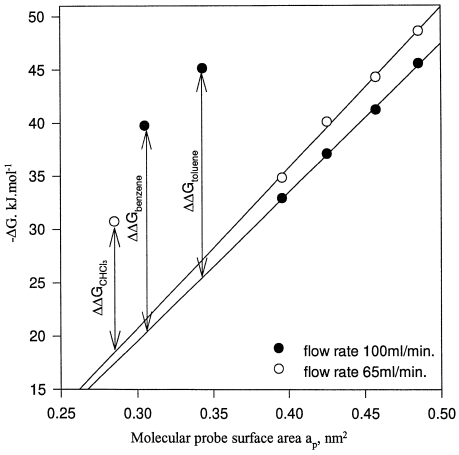

Fig. 2. The determination of specific interaction, NaX at 230°C.

$$I^{sp} = \frac{\Delta\Delta G}{N a_p} \quad (8)$$

The probe surface area a_p, in practice, can be calculated from the liquid density and the molecular weight of the probe [25]. This treatment is empirical, it allows a comparison of the specific interaction between a zeolite and an adsorbate by use of a unified scale.

The adsorption enthalpy (ΔH_{ads}) was determined from the slope of $-R\ln V_n$ vs. $1/T$ plot (Fig. 3a,b).

$$\Delta H_{ads} = -R\frac{d(\ln V_n)}{d\left(\frac{1}{T}\right)} \quad (9)$$

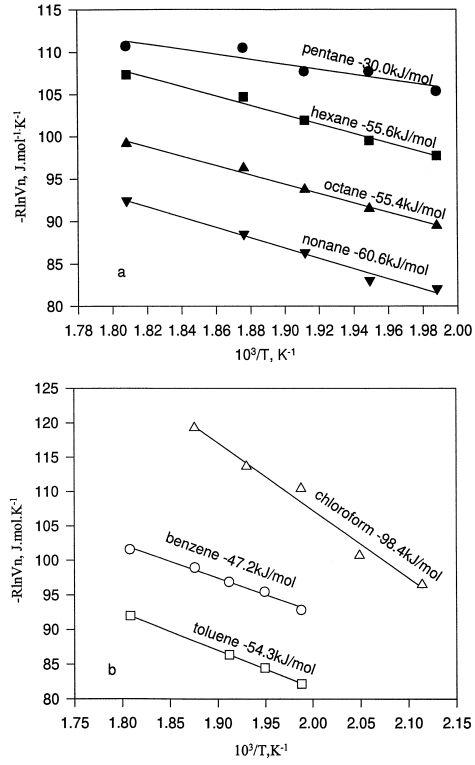

Fig. 3. The determination of adsorption enthalpies of probes on NaX zeolite.

4. Results and discussion

4.1. Diffusion of vapor probe molecules in zeolites

In order to measure specific interactions of probe molecules with polymer surfaces, Mukhopadhyay and Schreiber [26] and Qin and Schreiber [27] have discussed the contributions of probe adsorption on the external surface and probe diffusion within the bulk of the material. They have demonstrated that by changing the carrier gas flow rate and thus changing the contact time between adsorbate and adsorbent, it is possible to separate the surface adsorption contribution from the total retention datum. It may be expected that with microporous materials such as zeolites, this separation should be difficult and should command very restrictive experimental conditions. Thus, at the beginning of this work, a systematic research for the proper IGC conditions was performed. In order to reach small enough contact times, it was found necessary to use only a small column (20 mg of packing) and rather high carrier gas flow rates.

Fig. 4 shows, as an example, the variation of retention volume of the various probes studied with the change of flow rate at 260°C over the NaX column. It was observed that the retention volume V_n decreases with the increase of flow rate and levels off at higher flow rates. Similar results were also obtained by Mukhopadhyay and Schreiber [26] and Qin and Schreiber [27] in the case of polymers at temperatures higher than the glass transition T_g. They concluded that the increase in retention volume with the decrease of carrier gas flow rate is resulting from the increasing contribution of molecular diffusion. When the flow rate is high enough and does not affect the retention volume, it is considered that the probe diffusion within the particles is suppressed and the V_n value is the contribution of the surface adsorption of the probe molecule.

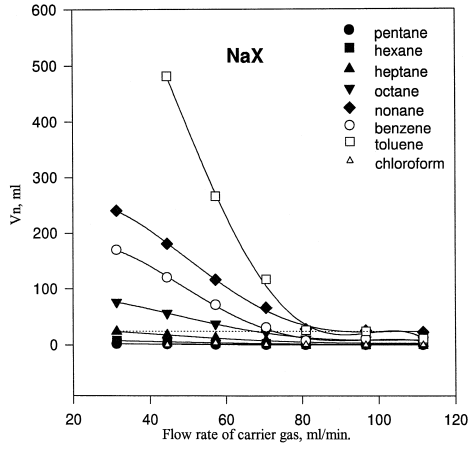

Fig. 4. The variation of retention volume with carried gas flow rate at 260°C, NaX.

Molecular diffusitivity is of course dependent on molecular dimensions and must, for example, decrease with the augmentation of the length of alkane chain. From Fig. 4, however it is clear that the contribution of diffusional effects to the retention volume increases with the alkane chain length. Similar results have been consistently reported in IGC of polymers [26,27]. In the present case, this behaviour reflects the fact that internal diffusion is not through free gas phase molecular diffusion but through surface mediated diffusion of the adsorbed phase. Thus, before they diffuse in, the probe molecules must first adsorb at the outer surface of the particles. Longer chain alkane molecules, being more strongly adsorbed, have longer contact time with the surface which gives them more time for internal diffusion. It is from Fig. 4 that, with this column, 100 ml/min was found to be a proper carrier gas flow rate for most probes utilized. At 65 ml/min, only pentane, hexane, heptane and chloroform have reached constant V_n.

4.2. Specific interaction

The interaction between a solid substrate and adsorbing species is attributed to secondary bonding caused by both polar and nonpolar (dispersive) Van der Waals forces between adsorbent and adsorbate. Fowkes [28,29] and Fowkes and Mostafa [30] have argued that these polar forces are actually Lewis acid–base inter-

actions. It is well known that zeolite samples have amphoteric properties, thus, in the present study of zeolite basicity, acid probe molecules, such as benzene and chloroform have been chosen for estimation of the basic strength of zeolites. Toluene was also studied for comparison with benzene because its alkylation reaction with methanol is one of the classical reactions catalyzed by alkali exchanged X-zeolites [31,32].

The adsorption of benzene on zeolites has been investigated mainly by De Mallmann and Barthomeuf [8–10], Dzwigaj et al. [11], Barthomeuf and De Mallmann [12], Su and Barthomeuf [13,14] and Su [15,16]. When benzene adsorbs on zeolites, there exist two kinds of adsorption sites, one is a Lewis acid site, that is the cation site interacting with the benzene ring (Fig. 5a). In this case, benzene is adsorbed on S_{II} and when possible, on S_{III} cations. The other sites are Lewis bases, namely, the zeolite framework oxygen atoms. According to Barthomeuf et al., benzene adsorbs on oxygen atoms of a 12-ring window (Fig. 5b). It may also be assumed that benzene could interact with one single basic oxygen as shown in Fig. 5c.

Our previous work revealed that the regular change in frequency of the NH (in the case of pyrrole) [7] and CH (in the case of chloroform) [17] bands observed upon exchange with alkali cations, can be associated to the variation in partial charges on zeolite framework oxygen atoms. Fig. 6a shows the variation of specific interaction (I^{sp}) between zeolites and the benzene probe at 230°C, 250°C and 280°C with the negative charge on zeolite framework oxygen atoms. This charge was calculated by means of the electronegativity equalization method [33,34]. The unit cell composition of zeolites (Table 1) was utilized in the EEM calculation of this average oxygen charge.

It is observed from Fig. 6a that the specific interactions between X-zeolites and benzene does not vary monotonously with the average negative charge on zeolite framework oxygen atoms. For LiX, the specific interaction is very high. Then, the Na form (NaX) shows a much smaller specific interaction with benzene. From NaX to RbX, the specific interaction increases almost linearly with the charge. In CsX however, the specific interaction is well below the line from NaX to RbX. Among the alkali metal cations, Li^+ has the strongest Lewis acidity. Thus, the decrease in I^{sp} from LiX to NaX suggests that the adsorption on the cations is predominant in LiX. In this case, the π_6^6 bond serves as electron donating system. Upon exchange with Na, K, and Rb, the Lewis acid strength diminishes and the Lewis basic strength of the oxygen atoms increases. Thus, this increasing specific interaction indicates that in this case, benzene interacts predominantly with the Lewis base sites. According to De Mallmann and Barthomeuf [9], Dzwigaj et al. [11]

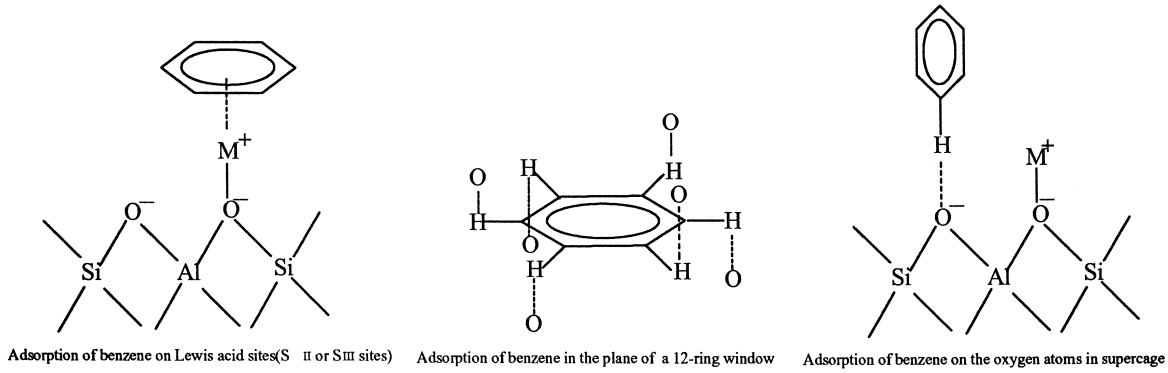

Fig. 5. The modes for benzene adsorbing on X-zeolites.

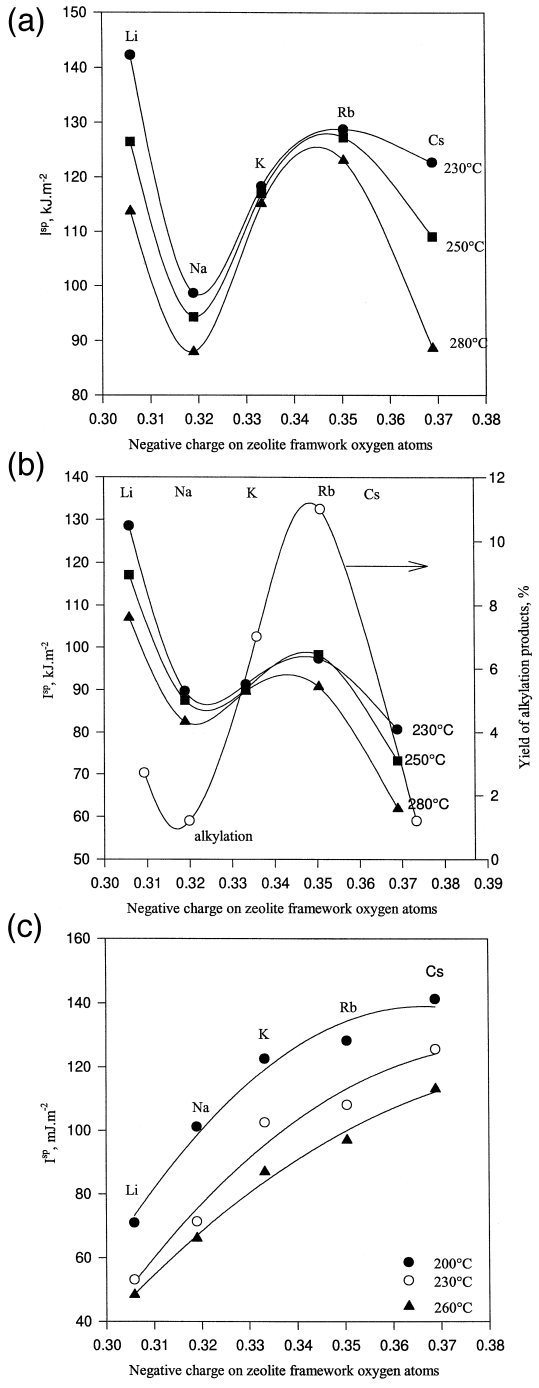

Fig. 6. (a) Specific interaction between X-zeolites and benzene as a function of the negative charge on zeolite framework oxygen atoms. (b) Specific interaction between X-zeolites and toluene variation with negative charge on zeolite framework oxygen atoms. (c) Variation of specific interaction between X-zeolites and chloroform with negative charge on zeolite framework oxygen atoms.

and Barthomeuf and De Mallmann [12], these sites should be oxygens of the 12R rings. It is thus quite surprising to observe (Fig. 6a) that CsX shows a smaller interaction with benzene than RbX. This result is not only reproducibly observed here, but similar results have also been observed for the interaction of toluene with the same solids (Fig. 6b). In order to understand this result, it may be recalled that basicity is a local property and that the basic oxygens in zeolites are those adjacent to one counter cation [7,18,19,21]. Thus, the benzene adsorption mode which involves the 12R window (Fig. 5b) must be stabilized by the migration of the counter cations to positions adjacent to the six oxygen atoms of the ring. Moreover, it is known that the mobility of the counter ions in zeolite decreases with their size [35]. It may thus be that the low mobility of the Cs^+ ion prevents the formation of the stable complex depicted in Fig. 5b on the time scale of the interaction at these high temperatures. Therefore, in spite of the higher electronic charge on the basic oxygens, the interaction with benzene would be smaller as it involves only one oxygen (as in Fig. 5c) instead of six (as in Fig. 5b)

The reaction of toluene with methanol has been widely studied and was often taken as a model reaction for testing the basicity or acidity of zeolites [31,32]. The selective formation of ethylbenzene and styrene is mainly dependent on the basicity of zeolites, while the ring alkylation reactions leading to xylenes are controlled by the acid sites zeolites. It is therefore specially meaningful to study the specific interactions of toluene with ion exchanged X-zeolites at the high temperatures allowed by IGC, in relation with the catalytic properties of these solids in the alkylation reaction.

Fig. 6b shows the variation of the specific interaction between toluene and zeolites at 230°C, 250°C and 280°C with the negative charge on zeolite framework oxygen atoms. These variations are very similar to the ones observed with benzene (compare Fig. 6a and b). They suggest that toluene is predominantly ad-

Table 2

Samples	LiX	NaX	KX	RbX	CsX
Specific interaction (I^{sp}, mJ/m^2) between zeolites and benzene at various temperatures					
230°C	142.2	98.6	118.3	128.7	122.7
250°C	126.5	94.3	117.0	127.3	109.1
280°C	113.1	87.9	115.1	123.1	88.6
Specific interaction between zeolites and toluene at various temperatures					
230°C	128.5	89.6	91.2	97.4	80.7
250°C	117.1	87.5	90.1	98.3	73.2
280°C	107.0	82.5	89.6	90.7	61.9
Specific interaction between zeolites and chloroform at various temperatures					
200°C	70.8	101.1	122.5	128.1	141.2
230°C	53.0	71.2	102.5	108.0	125.4
260°C	48.3	66.0	87.0	97.0	113.1

sorbed on LiX by interaction of the aromatic ring with Li^+ cations. It is interesting that Yashima et al. [31] report that over LiX, the methanol alkylation of toluene at 698 K yields essentially xylenes (Table 2). From the results in Fig. 6b, it is also seen that the specific interaction I^{sp} increases when Na^+ is exchanged for K^+ and Rb^+. This increase is, however, of lower amplitude than in the case of benzene which would be in line with the fact that in the case of toluene, only five hydrogen atoms interact with the 12R ring instead of 6 as in the case of benzene. Fig. 6b shows also the alkylation yield data of Yashima et al. [31], indicating a strong correlation with the measured I^{sp}. The selectivity for alkylation of toluene with methanol (Table 2) shows not only that over LiX zeolite, only xylenes are produced, but also that on KX, RbX, and CsX, no xylenes were detected, whereas all products appeared over NaX zeolite. These are also in perfect agreement with our interpretation of I^{sp} results according to which toluene interacts predominantly with the Lewis acid sites of LiX and with the basic acid sites of KX, RbX and CsX. Indeed, in this last case, only the base catalyzed side chain alkylation is observed. On NaX zeolite, both acid sites and Lewis base sites exist [32], thus, both side chain and ring alkylation occur. Even more interesting is the observed decreased yield for CsX which is essentially following the observed decreased I^{sp} of toluene.

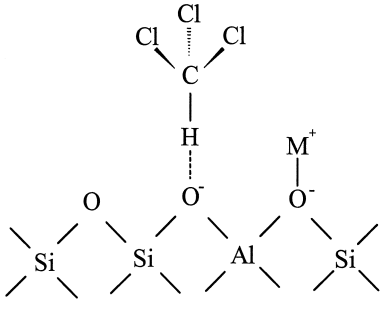

Fig. 7. The mode for chloroform adsorbing on zeolite basic sites [17,20].

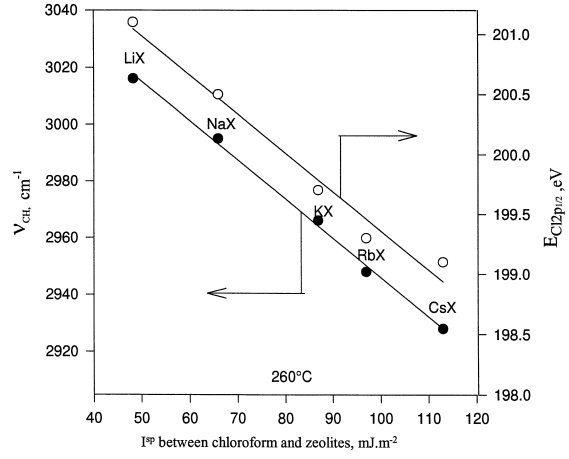

Fig. 8. The relationship between $I^{sp}_{chloroform}$ to ν_{CH} and $E_{Cl2p1/2}$.

Table 3
The results of Yashima's alkylation of toluene with methanol

Zeolites	Percent exchanged	Yield of products (%)				
		Ethylbenzene	Styrene	*o*-Xylene	*m*-Xylene	*p*-Xylene
LiX	75	0	0	1.1	0.4	1.2
NaX		0.1	0.5	0.36	0.05	0.19
KX	90	5.1	1.9	0	0	0
RbX	70	6.8	4.2	0	0	0
CsX	77	trace	1.2	0	0	0

Data were taken from Ref. [31], reaction condition: 698 K, $W/F = 25$ g (h/mol)$^{-1}$, mole ratio of toluene to methanol = 6:1

It is also worth mentioning that in the early work of Itoh et al. [36], it was found that toluene is more strongly adsorbed on acidic sites than on basic ones, which is also in agreement with the higher I^{sp} value observed on LiX.

In Refs. [17,20], it was shown that chloroform is a good probe for the study of basicity in zeolites. It was also shown that the most probable mode of adsorption involves the direct interaction of the H atom of chloroform with zeolites basic oxygens as depicted in Fig. 7. It had been long suspected that chloroform would decompose on very strongly basic sites [37]. Our previous FTIR study of chloroform $CHCl_3$ revealed that this molecule can indeed be decomposed when either the zeolite or chloroform itself contains traces of water. In the present work, anhydrous chloroform (Aldrich) was used as the probe molecule. The specific interaction of chloroform with the ion exchanged X-zeolite are given in Fig. 6c. Obviously, I^{sp} raises in the order $LiX < NaX < RbX < CsX$ which is exactly the order of increasing base strength of these alkali exchanged zeolites. This result is in perfect agreement with our previous FTIR [17], and XPS [20] studies which indicated that chloroform is a suitable probe for monitoring the basicity of these solids. Fig. 8 shows that the I^{sp} values obtained from IGC are indeed well correlated with both the ν_{CH} from FTIR and the binding energy $E_{Cl2p1/2}$ from XPS of chloroform chemisorbed on the same solids. (Table 3)

4.3. Enthalpies of adsorption

Table 4 shows the values of adsorption enthalpies for the *n*-alkanes and probe molecules over the various zeolites. These values where estimated using Eq. (9) and plots of $-R\ln V_n$ vs. $1/T$, examples of which are given in Fig. 3.

Eq. (9) is derived by replacing ΔG_{ads} by its expression Eq. (5) in the fundamental relation:

$$\Delta G_{ads} = \Delta H_{ads} - T\Delta S_{ads} \tag{10}$$

making the hypothesis of:

$$\frac{d(\Delta H_{ads})}{dT} = \frac{d(\Delta S_{ads})}{dT} = 0. \tag{11}$$

The calculated values of $-\Delta H_{ads}$ are reported in Fig. 9 as functions of the negative charge on framework oxygens. Here, several differences must be noted with the variations observed for I^{sp} in Fig. 6. For toluene, the

Table 4
The adsorption enthalpies of probes on zeolites (kJ mol^{-1})

Zeolite	Pentane	Hexane	Octane	Nonane	Benzene	Toluene	Chloroform
LiX	34.3	57.8	68.0	71.9	68.4	75.8	24.2
NaX	30.0	55.6	55.3	60.6	47.2	54.3	98.4
KX	70.3	52.6	61.1	76.1	42.7	66.9	74.6
RbX	60.9	52.2	74.2	72.8	74.8	88.5	65.0
CsX	18.5	60.7	71.4	91.3	92.3	83.1	56.0

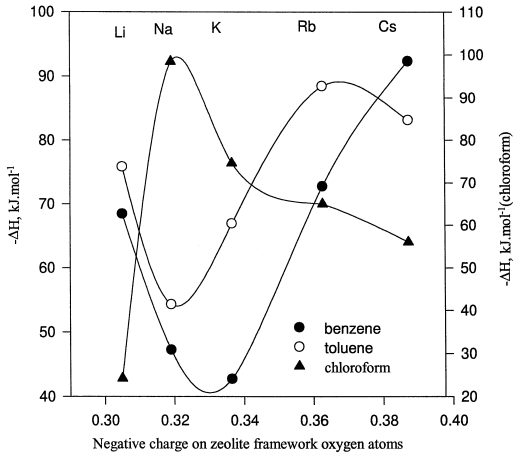

Fig. 9. The variation of adsorption enthalpies of benzene, toluene and chloroform on zeolites with the negative charge on zeolite framework oxygen atoms.

ΔH_{ads} curve is reminiscent of the I^{sp} curves in Fig. 6b. For benzene however, the lower Cs^+ I^{sp} value seen on Fig. 6a is not accompanied by a decreased $-\Delta H_{ads}$ for Cs compared to Rb. Moreover, whereas the I^{sp} values are higher for benzene than toluene, the $-\Delta H_{ads}$ values are clearly lower. In addition, the simple monotonous increase of chloroform I^{sp} with the oxygen charge is not observed for $-\Delta H_{ads}$. We believe that these differences reflect the fact that condition Eq. (11) is not met whenever the observed ΔG_{ads} $(-RT\ln V_n)$ is an average of several components including not only non-specific interactions and adsorption on a variety of different sites. In that case, the proportions of these various components change with temperature and consequently $-\Delta G_{ads}$ is a function of temperature. In such a case, the value estimated for ΔH_{ads} by Eq. (9) may be in large error.

5. Conclusion

This work shows that inverse gas chromatography is indeed a powerful and convenient method for the study and characterization of surface properties of zeolites. Provided the experimental conditions set by Mukhopadhyay and Schreiber [26] and Qin and Schreiber [27] where V_n is independent of the carrier gas flow rate are met, meaningful values are obtained for the specific interaction of probe molecules I^{sp}. These have the clear advantage of characterizing interactions at rather high temperatures, close to reaction conditions. It was, for example, found that dry chloroform is a very good probe molecule for characterizing zeolite base strength by IGC. The complex variations of benzene and toluene I^{sp} when zeolite X is alkali ion exchanged are in good agreement with the literature on the adsorption of these molecules and with the interpretation of selectivity and yields in toluene alkylation by methanol.

We found however that the ΔH_{ads} values derived from Eq. (9) are of doubtful value. This is likely associated to the fact that the various terms in ΔG_{ads} vary in different manners with temperature, in such a way that hypothesis Eq. (11) is not met and therefore, Eq. (9) is not valid in this case.

Moreover, we purposely did not report estimation of the non-specific interaction γ_s^D made using Eq. (6). We found these to vary in erratic manners. We believe that this is due to the fact that γ_s^D is dependent on the surface morphology of the particular sample under study. These estimations would therefore have no general significance.

Clearly, the meaningful information retrieved by IGC lies in the estimation of specific interactions I^{sp}.

Acknowledgements

The authors thank professor H.P. Schreiber for interesting discussions and NSERC for financial support.

References

[1] A.V. Kiselev, in: J.C. Giddings, R.A. Keller (Eds.), Advances in Chromatography, Marcel Dekker, New York, 1967.
[2] O. Smidsrød, J.E. Guillet, Macromolecules 2 (1969) 272.
[3] D.R. Lloyd, T.C. Ward, H.P. Schreiber, Inverse gas chromatography: characterization of polymers and other materi-

als, ACS Symposium Series 391, Am. Chem. Soc., Washington, DC, 1989.
[4] H. Darmstadt, C. Roy, S. Kaliaguine, Rubber Chem. Tech., in press.
[5] F. Miano, Colloid Surf. A: Physicochem. Eng. Aspects 110 (1996) 95.
[6] D. Barthomeuf, J. Phys. Chem. 88 (1984) 42.
[7] M. Huang, S. Kaliaguine, J. Chem. Soc. Faraday Trans. 88 (1992) 751.
[8] D. De Mallmann, D. Barthomeuf, J. Chem. Soc. Chem. Commun. (1986) 476.
[9] D. De Mallmann, D. Barthomeuf, Zeolites 8 (1988) 292.
[10] D. De Mallmann, D. Barthomeuf, J. Chem. Soc. Chem. Commun. (1989) 129.
[11] S. Dzwigaj, D. De Mallmann, D. Barthomeuf, J. Chem. Soc. Faraday Trans. 86 (1990) 431.
[12] D. Barthomeuf, A. De Mallmann, in: P.J. Grobet et al. (Eds.), Innovation in Zeolite Materials Science, Elsevier, Amsterdam, 1987, p. 365.
[13] B.-L. Su, D. Barthomeuf, Appl. Catal. A: Gen. 124 (1995) 81.
[14] B.-L. Su, D. Barthomeuf, Zeolites 13 (1993) 626.
[15] B.-L. Su, Zeolites 16 (1996) 75.
[16] B.-L. Su, Zeolites 16 (1996) 25.
[17] J. Xie, M. Huang, S. Kaliaguine, React. Kinet. Catal. Lett. 38 (1996) 217.
[18] M. Huang, A. Adnot, S. Kaliaguine, J. Am. Chem. Soc. 114 (1992) 10005.
[19] M. Huang, A. Adnot, S. Kaliaguine, J. Catal. 137 (1992) 322.
[20] J. Xie, M. Huang, S. Kaliaguine, Appl. Surf. Sci. 115 (1997) 157.
[21] M. Huang, S. Kaliaguine, M. Muscas, A. Auroux, J. Catal. 157 (1995) 266.
[22] A. Sayari, E. Crusson, S. Kaliaguine, J.R. Brown, Langmuir 7 (1991) 314.
[23] M.J. Wang, S. Wolff, J-B. Donnet, Rubber Chem. Technol. 64 (1991) 559.
[24] E.F. Meyer, J. Chem. Educ. 57 (1980) 120.
[25] E.F. Emmett, S. Brunauer, J. Am. Chem. Soc. 59 (1937) 1553.
[26] P. Mukhopadhyay, H.P. Schreiber, Macromolecules 26 (1993) 6391.
[27] R.-Y. Qin, H.P. Schreiber, Langmuir 10 (1994) 4153.
[28] F.M. Fowkes, Rubber Chem. Technol. 57 (1983) 328.
[29] F.M. Fowkes, J. Adhesion Sci. Technol. 1 (1987) 7.
[30] F.M. Fowkes, M.A. Mostafa, Ind. Eng. Chem. Prod. Res. Dev. 21 (1982) 337.
[31] T. Yashima, K. Sato, T. Hayasaka, N. Hara, J. Catal. 26 (1972) 303.
[32] J. Xie, S. Kaliaguine, Appl. Catal. A: Gen. 148 (1997) 415.
[33] R.T. Sanderson, Chemical Bonds and Bond Energy, Academic Press, New York, 1976.
[34] R.T. Sanderson, J. Am. Chem. Soc. 105 (1983) 2259.
[35] F.J. Jansen, R.A. Schoonheydt, J. Chem. Soc. Faraday Trans. 69 (1973) 1338.
[36] H. Itoh, A. Miyamoto, Y. Murakami, J. Catal. 64 (1980) 284.
[37] E.A. Paukshtis, N.S. Kotsarenko, L.G. Karakchiev, React. Kinet. Catal. Lett. 12 (1979) 315.